ACS APPLIED MATERIALS & INTERFACES

www.acsami.org

Research Article

Substrate-Independent Maskless Writing of Functionalized Microstructures Using CHic Chemistry and Digital Light Processing

Dan Song, Frederik Kotz-Helmer, Bastian Rapp,* and Jürgen Rühe*

Cite This: *ACS Appl. Mater. Interfaces* 2022, 14, 50288−50295

Read Online

ACCESS | Metrics & More | Article Recommendations | Supporting Information

ABSTRACT: Maskless photolithography based on digital light processing (DLP) is an attractive technique for the rapid, flexible, and cost-effective fabrication of complex structures with arbitrary surface profiles on the microscale. In this work, we introduce a new material system for structure formation by DLP that is based on photoreactive polymers for the local and light-induced C,H-insertion cross-linking (CHic). This approach allows a simple and versatile generation of microstructures with a broad spectrum of geometries and chemistries irrespective of the nature of the chosen substrates and thus allows direct writing of surface functionalization patterns with high spatial control. The CHicable prepolymer is first coated on a substrate to form a solvent-free (glassy) film, and then the DLP system patterns the light with arbitrary shape to induce local cross-linking of the prepolymer. Using this method, the desired structures with complex features with a lateral resolution of several microns and a topography of tens of nanometers could be fabricated within 30 s. Furthermore, the universal applicability of the CHic reaction enables the printing on a wide variety of substrates, which greatly broadens the using scenarios of this printing approach.

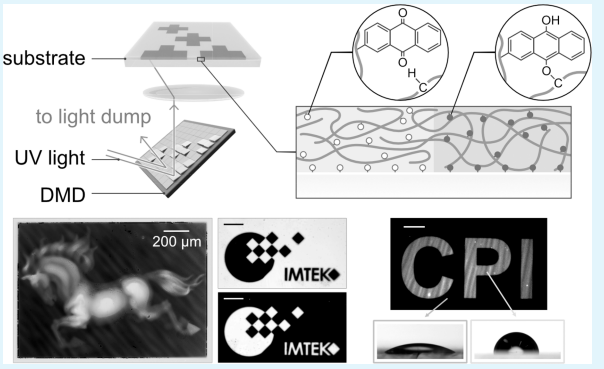

KEYWORDS: *photoreactive polymers, C,H insertion cross-linking, maskless photolithography, digital light processing, functional microstructures*

INTRODUCTION

Photocuring, which is commonly defined as the conversion of a liquid polymerizable resin to a stable solid through irradiation with light,[1] has been widely used in 2D and 3D printing applications. With photocurable resins, the fabrication of microstructures has increasingly attracted interest in both academia and industry. Over the past decades, significant efforts have been made in developing maskless technologies to fabricate microstructures at significantly reduced costs and increased flexibility.[2,3] Among them, one of the most promising maskless technologies is photolithography based on digital light processing (DLP).[4−6] DLP is a projection technology using a so-called digital micromirror device (DMD) as a spatial light modulator invented by Texas Instruments in 1987.[7] DMDs consist of an array of several hundred thousand microscopic mirrors which can be rotated in such a way that the light is either directed to a substrate or (in the dark mode) to a light dump. DMDs are convenient instruments for optical projection as they allow controlling each of these mirrors individually, thus generating computer-controlled light patterns in real time. A DMD projects a full frame at a time and thus allows photocuring of the entire layer simultaneously, allowing significant increases in throughput compared to, e.g., sequential scanning systems such as laser lithography systems.[8] Moreover, by addressing the individual mirrors via pulse-width modulation, grayscale patterns and structures with complex topographies can be created.[4,9−11]

DMD-based lithography has become a versatile tool in many fields in the past few decades; however, there is still a significant lack in the variety of photocurable resins. Conventional photocurable resins used in this field typically consist of photoinitiators that generate free radicals or react as photoacids when exposed to light, monomers that form the backbone of the polymer network, and various other additives, e.g., for modulating the light penetration depth.[12] Although polymerization is a fast and versatile reaction, polymerization-based systems have several limitations. For example, quality control of individually generated polymerization-induced printed objects is challenging, as many parameters vital for the component's properties, e.g., the average molecular weight as well as the molecular weight distribution, are difficult to

Received: July 12, 2022
Accepted: September 9, 2022
Published: October 26, 2022

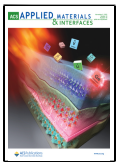

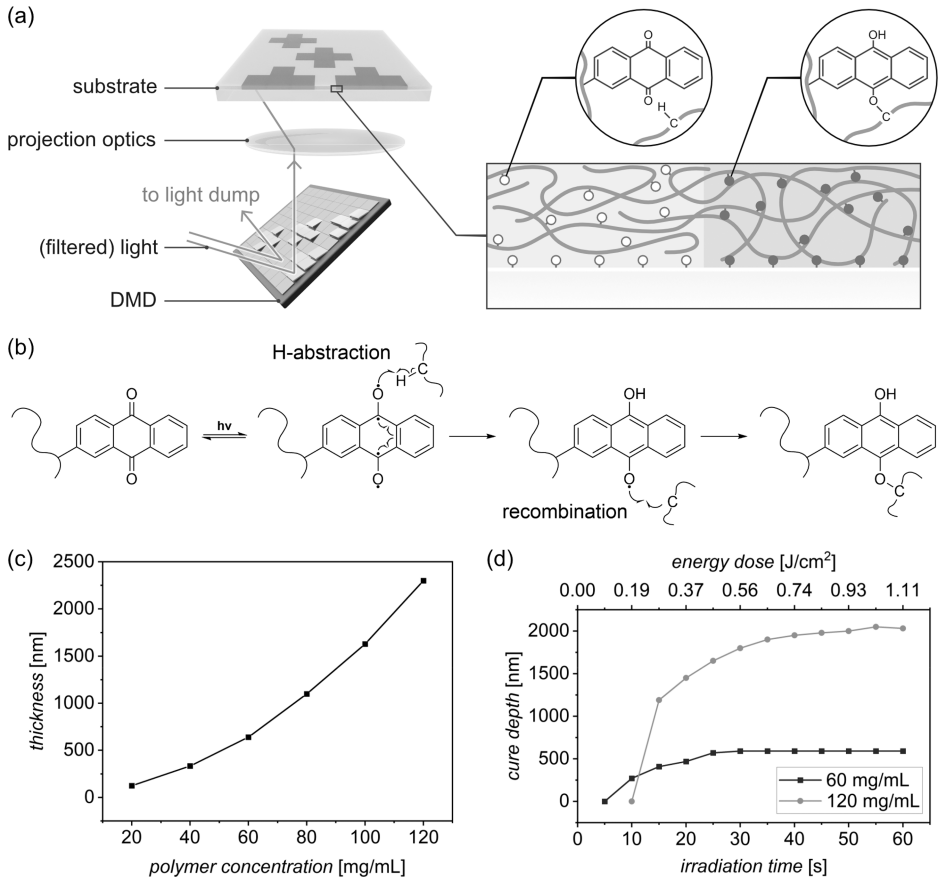

Figure 1. Digital light processing (DLP) of CHicable polymers. (a) Schematic representation of microstructuring via CHic reaction using the DMD-based projection lithography system. The unreacted anthraquinone units (○) can be activated by UV light and then cross-linked with neighboring C,H units on the polymer chains as well as on the substrate through the CHic reaction (●). Eventually, a surface-attached polymer network is formed. (b) Mechanism of the CHic reaction of anthraquinone containing polymers. The anthraquinone unit can be excited by UV light and form a reactive intermediate, the oxygen-centered biradical, which can abstract a hydrogen atom from a neighboring aliphatic molecule and generate two radicals. After recombination of the generated radicals, the biradical inserts itself into an adjacent aliphatic C,H bond.[22,31] (c) Correlation between the deposition thickness and polymer concentration of PMMA-*co*-AOAQ. (d) Cure depth in dependence of the energy dose for the polymer PMMA-*co*-AOAQ at two polymer concentrations. During the early stage, small variations in the energy dose lead to different cure depths (structure heights), which indicates the possibility of greyscale printing by modulating the exposure time of individual mirrors of the DMD.

control in such settings. Furthermore, the residual monomers, which are in most cases considered as a safety hazard, are often entrapped in the fabricated structures and leach out slowly during prolonged use, rendering the fabricated microstructures problematic of even unsuitable for many applications, e.g., in cell culture biology.[13−15]

In addition to the limitations stemming from the use of conventional photoresins themselves, the choice of possible substrates onto which the microstructures are printed is also limited because the microstructures fabricated from these photoresins attach to the surfaces only through physical adhesion. This leads frequently to problems such as delamination and insufficient long-term stability. In many applications such as optical waveguide devices as well as microelectromechanical systems (MEMS) used for sensors, actuators and molecular electronics, the generation of polymer patterns covalently bonded to inorganic substrates such as silicon is attracting increasing attention.[16,17] Besides, polymeric substrates have come in recent years much more into the focus of microtechnologies and flexible electronics due to their mechanical flexibility, low fabrication cost and good processability.[18,19] However, the adhesion issue is even worse for polymeric substrates. Printing of polymeric microstructures on polymer substrates is in almost all cases difficult, especially when nonpolar polymers are used, which are actually the majority of the used polymers. To enable functionalization, harsh processes such as flame treatment or corona treatment have been used to introduce reactive sites into the surface to which the polymer can be coupled. However, the degree of functionalization decreases with time, which is known as the aging phenomenon or hydrophobic recovery.[20]

To address the problems, in this work, we present a novel photoactive prepolymer system as a new negative-type photoresin. This prepolymer undergoes photoinduced C,H-insertion cross-linking (CHic) to form a polymer network. To this end, the prepolymers carry functional groups such as benzophenones, anthraquinones, and diazo compounds, which form reactive radicals or carbenes upon excitation by light. These reactive intermediate groups can react with aliphatic groups in neighboring macromolecules, eventually forming a cross-linked network.[21,22] The difference for classical monomer systems is that the "CHicable" systems consist of only one component: the prepolymer. The system is thus significantly simpler and requires no subsequent purification steps. After developing the unincorporated prepolymer chains, the fabricated microstructures are safe to use in a biological

https://doi.org/10.1021/acsami.2c12000
ACS Appl. Mater. Interfaces 2022, 14, 50288−50295

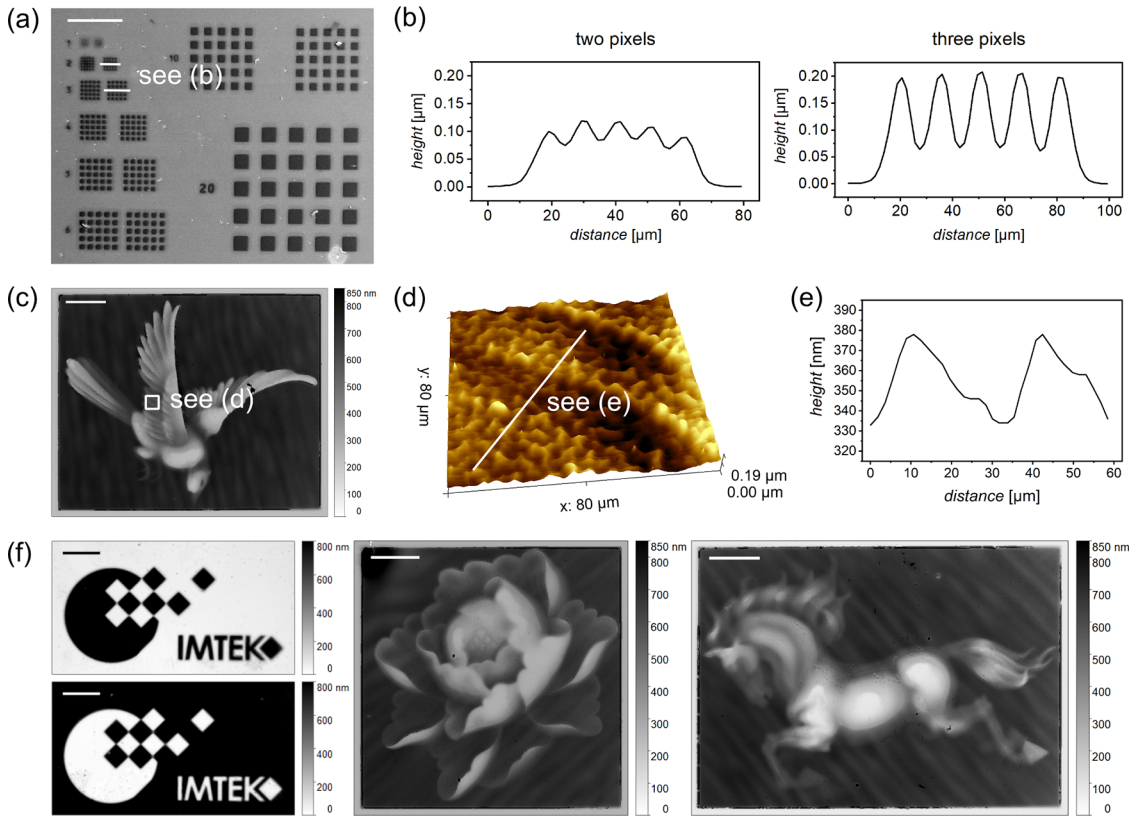

Figure 2. Microstructures of CHicable polymers generated via DLP. (a) SEM image of a binary test pattern generated from 60 mg mL^{-1} of PMMA-*co*-AOAQ exposed at 365 nm for 30 s. The test pattern consists of squares with widths ranging from 1 to 20 DMD pixels in width (2.5−50 μm). In every row, the width and distance between patterns are equal. (b) Height profiles of the squares with widths of two pixels and three pixels (see the marks in (a)) show that the smallest resolvable resolution is 5 μm (2 pixels). (c) WLI image of a grayscale bird generated via 30 s exposure at 365 nm and (d) the atomic force microscopy (AFM) image of an area of 80 × 80 μm^2 on the wing (see the mark in (c)). (e) Height profile of the line marked in (d), which crosses two pieces of feather on the wing, shows that relief surface topography at a scale of several tens of nanometers along axial direction can be printed clearly. (f) WLI images of the printed binary and grayscale microstructures. All structures were printed on the same glass slide coated with 60 mg mL^{-1} PMMA-*co*-AOAQ exposed at 365 nm in 30 s. All scale bars: 200 μm.

environment as the prepolymer is neither hazardous nor volatile.[23]

The most unique and advantageous feature of the CHic reaction is its universal applicability. Compared to other cross-linking strategies that need two functional groups for forming a covalent bond, CHic only requires aliphatic C,H units as reaction partners. Thus, all polymeric systems can potentially cross-link via CHic irrespective of the chemical nature of molecules. The microstructures created via CHic can be generated on and from a wide range of materials since the required C,H units are ubiquitous, including inorganic and polymeric substrates. Numerous covalent bonds are established at the interface, rendering a stable system. In addition, CHic is very robust as the reaction happens under a wide range of reaction conditions and is particularly insensitive to the presence of inhibitors such as oxygen, which are notorious sources of uncured material in classical negative-type photoresins.[24] Moreover, the process allows the simple incorporation of complex molecules, e.g., proteins, dyes, and DNA.[25,26] The incorporation can be easily realized either by copolymerization or by simply mixing the desired functional groups into the prepolymer.[25,26] This opens up possibilities to generate functional microstructures conveniently.

RESULTS AND DISCUSSION

In the present work, we combine the advantages of CHic chemistry and DLP technology using a custom-built DMD-based lithography system for the fabrication of binary and grayscale microstructures.[10,27] The overall process is shown in Figure 1a. The CHicable prepolymer is first coated on a substrate. After evaporation of the solvent, a homogeneous solvent-free film is formed. The DMD system then projects the incident UV light pattern following a digital bitmap to induce localized cross-linking and write the desired microstructure. After development with an appropriate solvent, the non-exposed and thus non-cross-linked prepolymer can be rinsed away.

We chose to use a copolymer of methyl methacrylate (MMA) and a small amount of acryloxyanthraquinone (AOAQ) as a photoreactive polymer for the layer formation. This copolymer can be synthesized in high yields by following a straightforward procedure (Figure S1a, Supporting Information). We used this polymer because poly(methyl methacrylate) (PMMA) has attracted significant interest for laboratory-scale rapid prototyping due to its prominence in microfluidics and biochips mostly due to its outstanding optical clarity and good biocompatibility.[28,29] AOAQs have been used as dyes and UV photoinitiators since the 1990s.[30] Recently, AOAQ moieties have been studied as a cross-linker for CHic systems as it shows fast photoreaction at low irradiation energy.[31]

https://doi.org/10.1021/acsami.2c12000
ACS Appl. Mater. Interfaces 2022, 14, 50288−50295

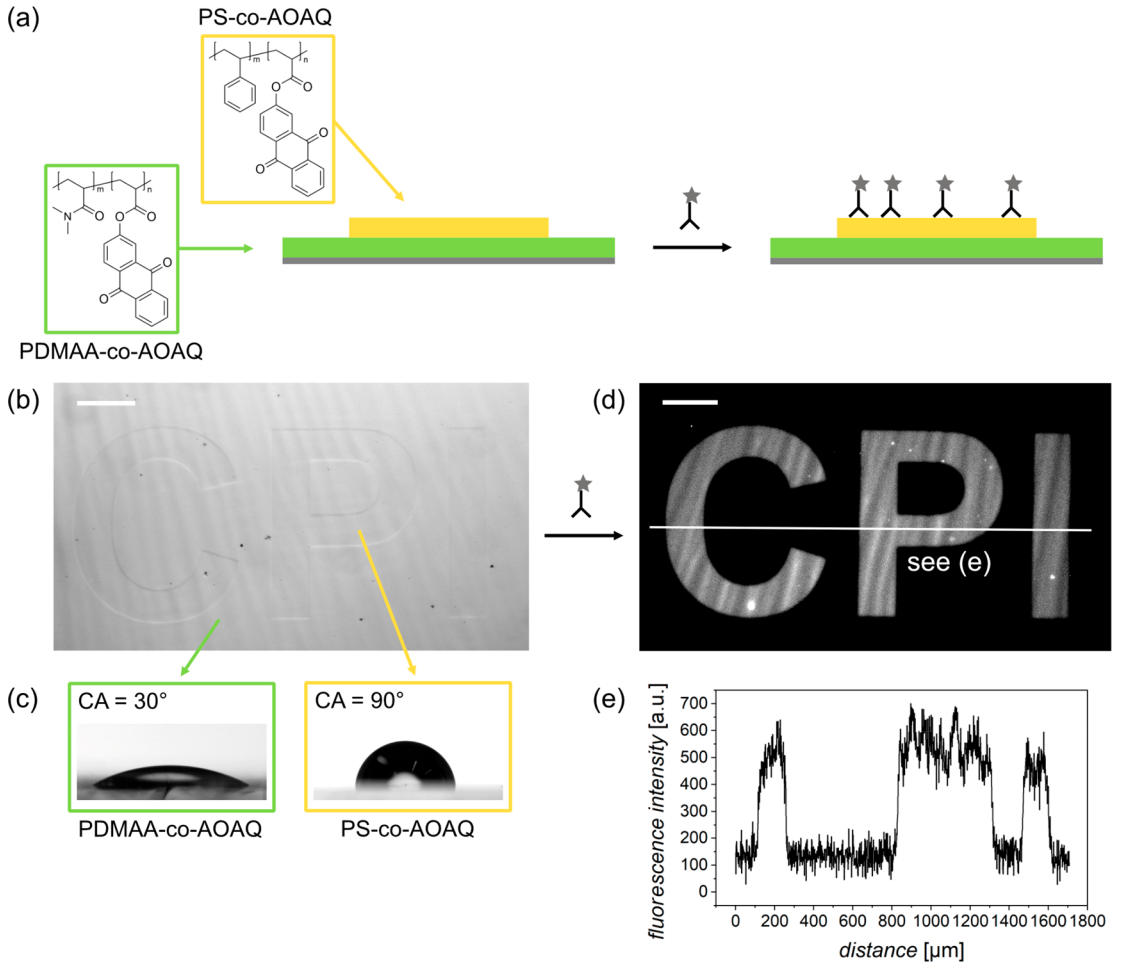

Figure 3. Patterns with spatially controlled protein adsorption. (a) Depiction of the generated two-layered pattern and the following protein incubation; the pattern consists of a whole layer generated from 60 mg mL^{-1} PDMAA-*co*-AOAQ on the bottom and a pattern from 60 mg mL^{-1} PS-*co*-AOAQ on top. (b) Optical microscope image of the fabricated two-layered pattern. (c) Contact angle measurement of surfaces bonded with PDMAA-*co*-AOAQ and PS-*co*-AOAQ, respectively. (d) Fluorescence microscope image of the two-layered pattern after incubation with fluorescently labeled proteins, and (e) the fluorescence intensity difference along the line that acrosses these two regions (see the mark in (d)). The proteins adsorb only in the regions where the hydrophobic polymer network is generated. All scale bars: 200 μm.

Figure 1b shows the process of the CHic reaction. When exposed to UV light, AOAQ shows adsorption in the range of 300−360 nm (Figure S2, Supporting Information), which corresponds to an n,π^* transition in the carbonyl unit.[21] This transition leads to a biradicaloid triplet state of the oxygen-centered radical, which can abstract a hydrogen atom from a neighboring aliphatic molecule. Subsequently, two radicals are generated after hydrogen abstraction. Through recombination of the generated radicals, the biradical can insert itself into any adjacent aliphatic C,H bond.[21] If the two reactants are located on different chains, a cross-linked network will eventually form.[22] The PMMA-*co*-AOAQ used in this study has a cross-linker content of 5 mol % and a molecular weight of approximately 173000 g mol^{-1}, which yields approximately 80 cross-linker units per chain. This number is more than sufficient to cross-link the polymer reaching the gel point rapidly even at a rather moderate conversion.[32]

The PMMA-*co*-AOAQ prepolymers were spin-coated from a toluene solution to form solvent-free (glassy) films on pretreated glass substrates. The deposition thickness increased with increasing polymer concentration (Figure 1c). After deposition, the samples were placed in the microlithography system and exposed to a UV light pattern. The cure depths were determined from the remaining thicknesses of the films on the projected area after a thorough development in toluene using a Soxhlet extractor. Such a developing procedure guarantees complete removal of the polymer chains that are not bound to the cross-linked network. Figure 1d shows the final film thickness as a dependence of the energy dose for films of PMMA-*co*-AOAQ deposited at concentrations of 60 and 120 mg mL^{-1}, which correspond to film thicknesses of approximately 530 and 2200 nm as shown in Figure 1c. During the early stage of curing, the prepolymer is only lightly cross-linked, so that chains that are not incorporated into the polymer network could be washed away during development. At this stage, small variations in the energy dose will change the extent and depth of the cross-linking process, which allows us to control the height of the structures. At the plateau stage, the film is completely cured and the thickness remains unchanged even if a higher energy dose is applied to the system.

Microstructures generated from PMMA-*co*-AOAQ by the described procedure are shown in Figure 2. To test the resolution of the photoreactive polymer printed by the DMD lithography system, a binary test pattern consisting of squares with widths ranging from 1 to 20 DMD pixels (5× objective),

https://doi.org/10.1021/acsami.2c12000
ACS Appl. Mater. Interfaces 2022, 14, 50288−50295

i.e., 2.5−50 μm, was created. On a pretreated glass slide, 60 mg mL^{-1} PMMA-*co*-AOAQ was spin-coated and projected by UV light at a wavelength of 365 nm for 30 s. The scanning electron microscopy (SEM) images of the generated microstructures are shown in Figure 2a. Squares with a width from two pixels (5 μm) to 20 pixels (50 μm) were well resolvable. Figure 2b shows the height profiles of squares having widths of two pixels (5 μm) and three pixels (7.5 μm). Two pixels, namely 5 μm, are the smallest structures that can be resolved. Here, the peak height decreases with decreasing pixel number because of the edge fanning out phenomenon which has been discussed in a previous publication.[33] Briefly, chains located at the edge of the pattern have a little bit of "freedom" and can fan out. If the pattern dimension is large (high pixel number), such edge effects affect only a small portion of all chains, namely those close to the edge of the pattern. However, if the pattern dimension is small (small pixel number), the relative proportion of such chains compared to the total number of chains increases, resulting in a lens-like morphology and a decrease in height.[33]

In addition to binary structures, we also generated grayscale microstructures. As aforementioned, to fabricate microstructures with various heights of CHicable polymers, the exposure dose should be precisely modulated. This can be realized in a straightforward way using the DMD-based photolithography system, which supports 8-bit grayscale encoding and thus (theoretically) 256 discrete structure heights. Combining CHicable materials and the DMD-based photolithography system thus enables the fabrication of grayscale microstructures via a single exposure. As an example, a grayscale image of a bird (Figure 2c) was fabricated from 60 mg mL^{-1} PMMA-*co*-AOAQ via exposure at 365 nm for 30 s. Figure 2d shows the surface topography recorded by atomic force microscope (AFM) of an area of 80 × 80 μm^2 on the image of a bird wing (see the mark in Figure 2c). To evaluate the height differences more precisely, Figure 2e shows the height profile obtained by the white light interferometry (WLI) of a line that crosses 2 pieces of feather on the wing (the position is marked in Figure 2d). As shown here, grayscale details at a scale of several tens of nanometers along the axial direction of the surface can be printed clearly. Additionally, to show the flexibility of this approach, several different binary and greyscale microstructures were fabricated on one substrate as shown in the WLI measurements in Figure 2f.

CHicable prepolymers can be conveniently designed to have various properties via copolymerization, which allows a great variability of the composition. Because the CHicable cross-linkers only require aliphatic C,H units as reaction partners, and then the reaction happens irrespective of the chemical nature of the used molecules, practically, all polymeric systems can cross-link via CHic and form films with different properties. To show this, we fabricated patterns that can be used to spatially control protein adsorption (Figure 3).

From previous studies, it is known that surface-attached swellable polymer networks prevent protein adsorption due to "entropic shielding", while proteins adsorb easily on most nonswellable polymer networks.[34,35] Therefore, the difference in swelling behavior can be utilized to generate regions with varying protein adsorption. As depicted in Figure 3a, a complete layer of PDMAA-*co*-AOAQ (PDMAA: poly(N,N-dimethylacrylamide)) was fabricated on a pretreated glass slide. To achieve this, a layer of PDMAA-*co*-AOAQ was spin-coated on the pretreated glass slide, exposed to UV light at 365 nm for 5 min, and then developed with ethanol. Subsequently, a layer of PS-*co*-AOAQ (PS: polystyrene) was spin-coated on top and printed by the presented approach (365 nm, 30 s). After developing with toluene, the not cross-linked material was washed away. Figure 3b shows an optical microscope image of the whole layer of PDMAA-*co*-AOAQ which is hydrophilic with a binary logo on top printed from PS-*co*-AOAQ which is hydrophobic. Figure 3c shows the contact angle data of surfaces bonded with these two polymers, respectively. After preparation of the two-layered sample, it was incubated with Alexa Fluor 647-conjugated AffiniPure Goat Anti-Human Serum IgA in phosphate buffered saline (PBS) for 1 h and washed thoroughly. The bright fluorescence emissions visible in the images depicted in Figure 3d show that proteins adsorb to the printed regions of nonswellable PS-*co*-AOAQ strongly. In contrast to this, the regions composed of swellable PDMAA-*co*-AOAQ do not adsorb proteins and remain dark. Figure 3e shows the fluorescence intensity difference between these two regions.

Furthermore, we employed different types of substrates to demonstrate that CHicable prepolymers can be conveniently microstructured on a wide range of materials. To get intact microstructures, it is critical to prevent delamination of the fabricated microstructures from the surface, especially during development. To achieve this, the establishment of covalent bonds between the microstructures and the solid surface is desirable. If the substrate itself is a polymer or a biomaterial that contains C,H groups, covalent bonds are conveniently established not only between the chains forming the network but also to the surface of the substrate. In this work, a PMMA substrate was employed as the polymeric substrate, and a substrate coated with a gelatin layer was used as the biomaterial-based substrate. In the case of inorganic substrates, C,H groups can be introduced by binding small molecules to the surface of the substrate. For this, we employed glass slide as the inorganic substrate and used triethoxyanthraquinonesilane (AQ-silane) to modify the glass surface. We have previously reported the two-step synthesis of the AQ-silane and its immobilization on glass substrates.[36] The silane layer contains anthraquinone groups identical to the groups in the polymer. Upon activation, the CHic reaction thus happens not only within the polymer itself but also between the polymer and the silane layer on the glass surface.

To visualize the printed microstructures, a fluorescently labeled CHicable prepolymer PDMAA-*co*-AOAQ-*co*-RAS (RAS: (rhodamine B isothiocyanate)-aminostyrene) was synthesized (Figure S1b, Supporting Information) as the prepolymer to be printed on different substrates as the dye allows visualization of the structures via fluorescence microscopy. The incorporated dye, rhodamine B isothiocyanate (RBITC) has a very low adsorption at 365 nm (Figure S3, Supporting Information). The resulting slight loss of intensity does not influence the cross-linking process as we are in a robust regime well above the percolation threshold. The fluorescently labeled prepolymer was spin-coated at a concentration of 60 mg mL^{-1} on each substrate and then illuminated by the DMD-based photolithography system. After developing with ethanol, only the illuminated regions showed a bright fluorescence emission indicating the presence of the cross-linked material. The nonexposed portion of the film was removed during development and thus remained dark. As shown in Figure 4, a binary logo was successfully printed on each of the three substrates demonstrating that the CHicable

https://doi.org/10.1021/acsami.2c12000
ACS Appl. Mater. Interfaces 2022, 14, 50288−50295

Figure 4. Fluorescence microscope images of microstructures produced with PDMAA-*co*-AOAQ-*co*-RAS on (a) PMMA (polymeric substrate), (b) glass slide (inorganic substrate), and (c) gelatin (biomaterial-based substrate). Scale bars: 200 μm.

materials can be printed on polymeric, inorganic, and biomaterial-based substrates.

CONCLUSIONS

In summary, we demonstrated that the use of CHicable prepolymers as a novel photocurable material in combination with DMD-based photolithography is a powerful and versatile tool for the rapid and flexible fabrication of binary and greyscale microstructures with surface features which can be freely defined. The material acts as a negative-type photoresin and allows the facile, maskless generation of complex surface profiles. Binary patterns with several microns resolution and surface-relief structures with topographic features as low as tens of nanometers can be fabricated via a single exposure. Since the curing mechanism is based on cross-linking of a polymeric network rather than polymerization of monomers, the microstructures are fabricated without the use of any low molecular weight compound that might leach out during use. This stronyl mitigates safety concerns, as leaching of such compounds could cause severe problems specifically in biological studies. The presented approach thus holds great promise for the fabrication of microstructures that are potentially suitable for biomedical use. In addition, as CHicable prepolymers can be conveniently synthesized with different properties, we demonstrated that this strategy allows for the customization of surface microstructures for specific applications, extending the application from mere topographical pattern to complex, functional microstructures.[23,36] We also demonstrated that these materials can be directly written onto a wide variety of substrates, including polymeric, inorganic, and biomaterial-based substrates while forming covalent bonds in each case. This significantly broadens the use scenario of microstructures made from such materials.

EXPERIMENTAL SECTION

Instrumentation. ^{1}H and ^{13}C NMR spectra were recorded on an Avance II 300 MHz NMR spectrometer (Bruker, USA). The gel permeation chromatography (GPC) measurements were carried out with an 1100 Series GPC-SEC system (Agilent, USA), and narrow polydispersity PMMA was used as the standard. The UV−vis spectroscopy was carried out by a Varian Cary Bio 50 UV−vis spectrometer (Agilent, USA). The fluorescence measurements were carried out with an Eclipse TS100 microscope (Nikon, Japan). The SEM images were taken with a FEI Scios 2 HiVac system (Thermo Fisher, USA). A NV500 White Light Interferometer (Zygo, USA) was used to carry out the thickness measurements and visualize the greyscale microstructures. A Delta 6RC Spin-coater (SÜSS MicroTec, Germany) was used for spin-coating of polymer solutions onto substrates, the substrates were spun with 1500 rpm for 30 s. Stratalinker UV cross-linker 2400 (Stratagene, USA) was used to illuminate the prepolymer coated on substrate (exposure intensity: 2.4 mW cm^{-2}). Contact angle measurements were carried out by OCA20 setup (DataPhysics, Germany) by dropping 10 μL of deionized water on substrate. A TS100F inverted optical microscope (Nikon, Japan) was used for imaging the fabricated microstructures. A JPK NanoWizard AFM system (Bruker, USA) was used to determine the surface topology.

Synthesis of Triethoxyanthraquinonesilane (AQ-silane). In the first step, 2-hydroxyanthraquinone (4.48 g, 0.02 mol, TCI, Germany) and potassium carbonate (4.14 g, 0.03 mol, 1.5 equiv, Carl Roth, Germany) were suspended in anhydrous acetone (30 mL, Sigma-Aldrich, USA), and allyl bromide (2.6 mL, 3.6 g, 0.03 mol, Sigma-Aldrich, USA) was added. Then 30 mL of water was added to the mixture after overnight refluxing and cooling to room temperature. The solution was extracted with diethyl ether (2 × 100 mL, Sigma-Aldrich, USA) which was then washed with dilute NaOH solution (10%). The organic phase was dried over Na_2SO_4 and filtered off. After removing the solvent, the obtained 2-allyloxyanthraquinone was recrystallized from methanol (Carl Roth, Germany). In the second step, freshly distilled triethoxysilane (30 mL, 26.7 g, 162 mmol, Sigma-Aldrich, USA) was mixed with Pt−C (0.002 g, 10% Pt) and 2-allyloxyanthraquinone (1.2 g, 4.6 mmol). The reaction mixture was then heated to reflux under nitrogen overnight. The residual triethoxysilane was removed via distillation. Pt−C was removed by filtration.

Synthesis of 2-Acryloxyanthraquinone (2-AOAQ). 2-Hydroxyanthraquinone (4 g; 17.84 mmol; 1 equiv) was first suspended in dichloromethane (350 mL, Carl Roth, Germany) and cooled with an ice bath. Triethylamine (Sigma-Aldrich, USA) was distilled from calcium hydride and added (4.8 mL; 35.68 mmol; 2 equiv); a homogeneous solution was then obtained. Acryloyl chloride (4.3 mL; 53.52 mmol; 3 equiv, Sigma-Aldrich, USA) was dissolved in dichloromethane (30 mL) and added dropwise to the solution. After the reaction mixture was stirred overnight at room temperature, the solid was filtered and washed several times with hydrochloric acid (0.1 M, Sigma-Aldrich, USA), saturated $NaHCO_3$ solution (Sigma-Aldrich, USA), and water, and recrystallized from ethanol (Carl Roth, Germany). ^{1}H NMR (300 MHz, $CDCl_3$, δ): 8.27−8.38 (m, 3H, Ar H), 8.06 (d, J = 3 Hz, 1H; Ar H), 7.77−7.84 (m, 2H, Ar H), 7.58 (dd, J = 9 Hz, 3 Hz, 1H; Ar H), 6.69 (dd, J = 18 Hz, 1 Hz, 1H; CH═CH_2), 6.37 (dd, J = 18 Hz, 12 Hz, 1H; CH═CH_2), 6.12 (dd, J = 9 Hz, 1 Hz, 1H; CH═CH_2). ^{13}C NMR (300 MHz, $CDCl_3$, δ): 182.3 (C═O), 182.1 (C═O), 163.6 (OC = O), 155.2 (C_{ar}O), 135.2 (C_{ar}C═O), 134.4 (C_{ar}), 134,2 (C_{ar}), 133,9 (C_{ar}C═O), 133,5 (C_{ar}C═O), 133.4 (CH═CH_2), 131.1 (C_{ar}), 129.4 (C_{ar}C═O), 127.4 (CH═CH_2), 127.3 (2C_{ar}), 127.2 (C_{ar}), 120.1 (C_{ar}).

Polymer Synthesis. The polymers were synthesized through statistical free-radical copolymerization. Methyl methacrylate (MMA, Sigma-Aldrich, USA) and *N*,*N*-dimethylacrylamide (DMAA, Sigma-Aldrich, USA) were purified via filtration with basic aluminum oxide (Sigma-Aldrich, USA) and distillation. 2,2′-Azobis(2-methylpropionitrile) (AIBN, Sigma-Aldrich, USA) was recrystallized from ethanol. For PMMA-*co*-AOAQ, MMA (4.1 mL, 3.8 g, 38 mmol) was dissolved with 2-AOAQ (0.56 g, 2 mmol) under nitrogen in dimethylformamide (DMF, Sigma-Aldrich, USA). The reaction was initiated with AIBN (0.04 mmol) and carried out at 60 °C for 16−20 h in DMF under nitrogen after three freeze and thaw cycles. The polymer was precipitated by adding it dropwise to a 10−15-fold excess of methanol and then filtered off. The polymer was purified through repeated dissolving and precipitating. The yield was approximately 55% (2.4 g). The amount of AOAQ in the copolymer was calculated from the ^{1}H NMR spectra to be 5.5 mol %, and the molecular weight was 173000 g mol^{-1} with a polydispersity of 2.8. In the same manner, styrene (4.4 mL, 3.98 g, 38 mmol) was dissolved with 2-AOAQ (0.56 g, 2 mmol) to yield 51% (2.3 g) PS-*co*-AOAQ, the amount of AOAQ in the copolymer was around 5 mol %, and the molecular weight was 65000 g mol^{-1} with a polydispersity of 2. DMAA (3.92 mL, 3.77 g, 38 mmol) was dissolved with 2-AOAQ (0.56 g, 2 mmol) to yield 58% (2.5 g) PDMAA-*co*-AOAQ, the amount of AOAQ in the copolymer was around 5 mol %, and the molecular weight was 40 000 g mol^{-1} with a polydispersity of 3.7. For the fluorescent-labeled polymer PDMAA-*co*-AOAQ-*co*-RAS, DMAA (3.88 mL, 3.73 g, 37.6 mmol), 2-AOAQ (0.56 g, 2 mmol), 4-aminostyrene (0.0476 g, 0.4 mmol, Sigma-Aldrich, USA), and AIBN (0.08 mmol) were dissolved. After copolymerization, RBITC (0.0032 g, 0.006 mmol, Sigma-Aldrich,

https://doi.org/10.1021/acsami.2c12000
ACS Appl. Mater. Interfaces 2022, 14, 50288−50295

USA) was added and the solution was shaken for 3 h. The polymer was then purified through repeated dissolving and precipitating. The yield was approximately 31% (1.36 g). The molecular weight was 14000 g mol^{-1} with a polydispersity of 2.8.

Sample Preparation. Glass slides were pretreated through spin-coating with AQ-silane solution and then heated to 120 °C for 20 min. As biomaterial-based substrates, gelatin powder (RUF Lebensmittelwerk, Germany) was thoroughly mixed with hot water, and the solution was then poured onto glass slides. After cooling overnight, the gelatin layers turned to dry films on the glass slides. CHicable prepolymer solutions (PMMA-*co*-AOAQ in toluene or PDMAA-*co*-AOAQ-*co*-RAS in ethanol) were then spin-coated on these slides and exposed by the custom-made lithography system at 365 nm. For the two-layered patterns, first, the PDMAA-*co*-AOAQ solution (60 mg mL^{-1} in ethanol) was spin-coated on a pretreated glass slide and exposed in the Stratalinker at 365 nm for 5 min. The PS-*co*-AOAQ solution (60 mg mL^{-1} in toluene) was then spin-coated on top to be exposed by the custom-made lithography system at 365 nm. Afterward, to ensure the complete removal of the un-cross-linked polymer chains, the substrates were developed for 16−20 h in a Soxhlet extractor with appropriate solvents—toluene for glass slides and PS-*co*-AOAQ layer, ethanol for PMMA substrates, gelatin, and PDMAA-*co*-AOAQ layer. After developing, the microstructures were characterized by SEM, WLI, and fluorescence microscopy.

Lithography. A custom-build microlithography system based on a DMD, which we have previously described, was used for cross-linking the CHicable prepolymers.[10,27,29] The desired microstructures were predesigned by the software GNU Image Manipulation Program as 8-bit digital bitmap images, which were parsed by a custom-written software to control the DMD to generate the corresponding UV light pattern, which was reflected to the demagnifying projection optics and then projected onto the substrate coated with the prepolymer. CHicable polymers were illuminated with a wavelength of 365 nm for 30 s (exposure intensity: 18.5 mW cm^{-2}).

Protein Incubation. The substrate with a two-layered pattern was incubated with a solution of Alexa Fluor 647-conjugated AffiniPure Goat Anti-Human Serum IgA in PBS for 1 h. The sample was then washed with PBS three times and determined by fluorescence microscopy.

■ ASSOCIATED CONTENT

Supporting Information

The Supporting Information is available free of charge at https://pubs.acs.org/doi/10.1021/acsami.2c12000.

Synthetic route of the photoactive acryloxyanthraquinone (AOAQ) monomer (Figure S1) and UV-vis spectra of PMMA-co-AOAQ irradiated at 365 nm and rhodamine B isothiocyanate (Figures S2 and S3) (PDF)

■ AUTHOR INFORMATION

Corresponding Authors

Bastian Rapp − *livMatS @ Freiburg Center for Interactive Materials and Bioinspired Technologies (FIT), University of Freiburg, 79110 Freiburg, Germany; Department of Microsystems Engineering (IMTEK), University of Freiburg, 79110 Freiburg, Germany;* orcid.org/0000-0002-3955-0291; Email: Bastian.Rapp@neptunlab.org

Jürgen Rühe − *livMatS @ Freiburg Center for Interactive Materials and Bioinspired Technologies (FIT), University of Freiburg, 79110 Freiburg, Germany; Department of Microsystems Engineering (IMTEK), University of Freiburg, 79110 Freiburg, Germany;* orcid.org/0000-0002-2534-8228; Email: ruehe@imtek.uni-freiburg.de

Authors

Dan Song − *livMatS @ Freiburg Center for Interactive Materials and Bioinspired Technologies (FIT), University of Freiburg, 79110 Freiburg, Germany; Department of Microsystems Engineering (IMTEK), University of Freiburg, 79110 Freiburg, Germany*

Frederik Kotz-Helmer − *Department of Microsystems Engineering (IMTEK), University of Freiburg, 79110 Freiburg, Germany*

Complete contact information is available at: https://pubs.acs.org/10.1021/acsami.2c12000

Notes

The authors declare no competing financial interest.

■ ACKNOWLEDGMENTS

This work was funded through the Cluster of Excellence Living, Adaptive and Energy-autonomous Materials Systems (livMatS) by the Deutsche Forschungsgemeinschaft (German Research Foundation) under Germany's Excellence Strategy EXC-2193/1-390951807. This project has received partial funding from the European Research Council (ERC) under the European Union's Horizon 2020 research and innovation program (Grant Agreement No. 816006). This work is also supported by the Research Cluster "Interactive and Programmable Materials (IPROM)" funded by the Carl Zeiss Foundation. The authors thank Prof. H. Zappe for the use of the WLI. Natalia Schatz is thanked for her help with synthesis. Michal Rössler is thanked for help with the schematics.

■ REFERENCES

(1) Phillips, R. Photopolymerization. *J. Photochem.* **1984**, *25*, 79−82.

(2) Kim, C.-S.; Ahn, S.-H.; Jang, D.-Y. Review: Developments in Micro/Nanoscale Fabrication by Focused Ion Beams. *Vacuum* **2012**, *86* (8), 1014−1035.

(3) Bushunov, A. A.; Tarabrin, M. K.; Lazarev, V. A. Review of Surface Modification Technologies for Mid-Infrared Antireflection Microstructures Fabrication. *Laser Photonics Rev.* **2021**, *15* (5), 2000202.

(4) Song, S.-H.; Kim, K.; Choi, S.-E.; Han, S.; Lee, H.-S.; Kwon, S.; Park, W. Fine-Tuned Grayscale Optofluidic Maskless Lithography for Three-Dimensional Freeform Shape Microstructure Fabrication. *Opt. Lett.* **2014**, *39* (17), 5162.

(5) Gauthier, G.; Lenton, I.; McKay Parry, N.; Baker, M.; Davis, M. J.; Rubinsztein-Dunlop, H.; Neely, T. W. Direct Imaging of a Digital-Micromirror Device for Configurable Microscopic Optical Potentials. *Optica* **2016**, *3* (10), 1136.

(6) Deng, Q.; Yang, Y.; Gao, H.; Zhou, Y.; He, Y.; Hu, S. Fabrication of Micro-Optics Elements with Arbitrary Surface Profiles Based on One-Step Maskless Grayscale Lithography. *Micromachines* **2017**, *8* (10), 314.

(7) Dudley, D.; Duncan, W. M.; Slaughter, J. Emerging Digital Micromirror Device (DMD) Applications. *SPIE MOEMS-MEMS* **2003**, 14.

(8) Malinauskas, M.; Žukauskas, A.; Purlys, V.; Gaidukevičiūtė, A.; Balevičius, Z.; Piskarskas, A.; Fotakis, C.; Pissadakis, S.; Gray, D.; Gadonas, R.; Vamvakaki, M.; Farsari, M. 3D Microoptical Elements Formed in a Photostructurable Germanium Silicate by Direct Laser Writing. *Opt. Lasers Eng.* **2012**, *50* (12), 1785−1788.

(9) Totsu, K.; Fujishiro, K.; Tanaka, S.; Esashi, M. Fabrication of Three-Dimensional Microstructure Using Maskless Gray-Scale Lithography. *Sens. Actuators Phys.* **2006**, *130*−*131*, 387−392.

(10) Waldbaur, A.; Waterkotte, B.; Schmitz, K.; Rapp, B. E. Maskless Projection Lithography for the Fast and Flexible Generation of Grayscale Protein Patterns. *Small* **2012**, *8* (10), 1570−1578.

(11) Norris, S. C. P.; Tseng, P.; Kasko, A. M. Direct Gradient Photolithography of Photodegradable Hydrogels with Patterned Stiffness Control with Submicrometer Resolution. *ACS Biomater. Sci. Eng.* **2016**, *2* (8), 1309−1318.
(12) Ligon, S. C.; Liska, R.; Stampfl, J.; Gurr, M.; Mülhaupt, R. Polymers for 3D Printing and Customized Additive Manufacturing. *Chem. Rev.* **2017**, *117* (15), 10212−10290.
(13) Gautam, R.; Singh, R. D.; Sharma, V. P.; Siddhartha, R.; Chand, P.; Kumar, R. Biocompatibility of Polymethylmethacrylate Resins Used in Dentistry. *J. Biomed. Mater. Res. B Appl. Biomater* **2012**, *100B* (5), 1444−1450.
(14) Krifka, S.; Spagnuolo, G.; Schmalz, G.; Schweikl, H. A Review of Adaptive Mechanisms in Cell Responses towards Oxidative Stress Caused by Dental Resin Monomers. *Biomaterials* **2013**, *34* (19), 4555−4563.
(15) Kloukos, D.; Pandis, N.; Eliades, T. Bisphenol-A and Residual Monomer Leaching from Orthodontic Adhesive Resins and Polycarbonate Brackets: A Systematic Review. *Am. J. Orthod. Dentofacial Orthop* **2013**, *143* (4), S104−S112.e2.
(16) Krogstad, J. A.; Keimel, C.; Hemker, K. J. Emerging Materials for Microelectromechanical Systems at Elevated Temperatures. *J. Mater. Res.* **2014**, *29* (15), 1597−1608.
(17) Park, T.-H.; Kim, S.-M.; Oh, M.-C. Polymer-Waveguide Bragg-Grating Devices Fabricated Using Phase-Mask Lithography. *Curr. Opt. Photonics* **2019**, *3* (5), 401−407.
(18) Gu, X.; Shaw, L.; Gu, K.; Toney, M. F.; Bao, Z. The Meniscus-Guided Deposition of Semiconducting Polymers. *Nat. Commun.* **2018**, *9* (1), 534.
(19) Ramadan, K. S.; Sameoto, D.; Evoy, S. A Review of Piezoelectric Polymers as Functional Materials for Electromechanical Transducers. *Smart Mater. Struct* **2014**, *23* (3), 033001.
(20) Jokinen, V.; Suvanto, P.; Franssila, S. Oxygen and Nitrogen Plasma Hydrophilization and Hydrophobic Recovery of Polymers. *Biomicrofluidics* **2012**, *6* (1), 016501.
(21) Prucker, O.; Brandstetter, T.; Rühe, J. Surface-Attached Hydrogel Coatings via C,H-Insertion Crosslinking for Biomedical and Bioanalytical Applications (Review). *Biointerphases* **2018**, *13* (1), 010801.
(22) Schuler, A.-K.; Prucker, O.; Rühe, J. On the Generation of Polyether-Based Coatings through Photoinduced C,H Insertion Crosslinking. *Macromol. Chem. Phys.* **2016**, *217* (13), 1457−1466.
(23) Kojima, T.; Husari, A.; Dieterle, M. P.; Fontaine, S.; Prucker, O.; Tomakidi, P.; Rühe, J. PnBA/PDMAA-Based Iron-Loaded Micropillars Allow for Discrete Cell Adhesion and Analysis of Actuation-Related Molecular Responses. *Adv. Mater. Interfaces* **2020**, *7* (7), 1901806.
(24) Ligon, S. C.; Husár, B.; Wutzel, H.; Holman, R.; Liska, R. Strategies to Reduce Oxygen Inhibition in Photoinduced Polymerization. *Chem. Rev.* **2014**, *114* (1), 557−589.
(25) Yodmongkol, S.; Sutapun, B.; Praphanphoj, V.; Srikhirin, T.; Brandstetter, T.; Rühe, J. Fabrication of Protein Microarrays for Alpha Fetoprotein Detection by Using a Rapid Photo-Immobilization Process. *Sens. Bio-Sens. Res.* **2016**, *7*, 95−99.
(26) Schönberg, J.-N.; Zinggeler, M.; Fosso, P.; Brandstetter, T.; Rühe, J. One-Step Photochemical Generation of Biofunctionalized Hydrogel Particles via Two-Phase Flow. *ACS Appl. Mater. Interfaces* **2018**, *10* (46), 39411−39416.
(27) Waldbaur, A.; Carneiro, B.; Hettich, P.; Wilhelm, E.; Rapp, B. E. Computer-Aided Microfluidics (CAMF): From Digital 3D-CAD Models to Physical Structures within a Day. *Microfluid. Nanofluidics* **2013**, *15* (5), 625−635.
(28) Hashimoto, M.; Barany, F.; Soper, S. A. Polymerase Chain Reaction/Ligase Detection Reaction/Hybridization Assays Using Flow-through Microfluidic Devices for the Detection of Low-Abundant DNA Point Mutations. *Biosens. Bioelectron* **2006**, *21* (10), 1915−1923.
(29) Kotz, F.; Arnold, K.; Wagner, S.; Bauer, W.; Keller, N.; Nargang, T. M.; Helmer, D.; Rapp, B. E. Liquid PMMA: A High Resolution Polymethylmethacrylate Negative Photoresist as Enabling Material for Direct Printing of Microfluidic Chips. *Adv. Eng. Mater.* **2018**, *20* (2), 1700699.
(30) Allen, N. S.; Hurley, J. P.; Bannister, D.; Follows, G. W. Photochemical crosslinking of nylon-6,6 induced by 2-substituted anthraquinones. *Eur. Polym. J.* **1992**, *28*, 1309.
(31) Schuler, A.-K.; Rother, R.; Prucker, O.; Müller, C.; Reinecke, H.; Rühe, J. A Novel Reactive Lamination Process for the Generation of Functional Multilayer Foils for Optical Applications. *Procedia Technol.* **2014**, *15*, 147−155.
(32) Kanokwijitsilp, T.; Körner, M.; Prucker, O.; Anton, A.; Lübke, J.; Rühe, J. Kinetics of Photocrosslinking and Surface Attachment of Thick Polymer Films. *Macromolecules* **2021**, *54* (13), 6238−6246.
(33) Chen, W.-L.; Menzel, M.; Prucker, O.; Wang, E.; Ober, C. K.; Rühe, J. Morphology of Nanostructured Polymer Brushes Dependent on Production and Treatment. *Macromolecules* **2017**, *50* (12), 4715−4724.
(34) Toomey, R.; Freidank, D.; Rühe, J. Swelling Behavior of Thin, Surface-Attached Polymer Networks. *Macromolecules* **2004**, *37* (3), 882−887.
(35) Wörz, A.; Berchtold, B.; Moosmann, K.; Prucker, O.; Rühe, J. Protein-Resistant Polymer Surfaces. *J. Mater. Chem.* **2012**, *22* (37), 19547.
(36) Schwärzle, D.; Hou, X.; Prucker, O.; Rühe, J. Polymer Microstructures through Two-Photon Crosslinking. *Adv. Mater.* **2017**, *29* (39), 1703469.

https://doi.org/10.1021/acsami.2c12000
ACS Appl. Mater. Interfaces 2022, 14, 50288−50295